ARTICLES

Editing-defective tRNA synthetase causes protein misfolding and neurodegeneration

Jeong Woong Lee[1], Kirk Beebe[2], Leslie A. Nangle[2], Jaeseon Jang[1]†, Chantal M. Longo-Guess[1], Susan A. Cook[1], Muriel T. Davisson[1], John P. Sundberg[1], Paul Schimmel[2] & Susan L. Ackerman[1,3]

Misfolded proteins are associated with several pathological conditions including neurodegeneration. Although some of these abnormally folded proteins result from mutations in genes encoding disease-associated proteins (for example, repeat-expansion diseases), more general mechanisms that lead to misfolded proteins in neurons remain largely unknown. Here we demonstrate that low levels of mischarged transfer RNAs (tRNAs) can lead to an intracellular accumulation of misfolded proteins in neurons. These accumulations are accompanied by upregulation of cytoplasmic protein chaperones and by induction of the unfolded protein response. We report that the mouse sticky mutation, which causes cerebellar Purkinje cell loss and ataxia, is a missense mutation in the editing domain of the alanyl-tRNA synthetase gene that compromises the proofreading activity of this enzyme during aminoacylation of tRNAs. These findings demonstrate that disruption of translational fidelity in terminally differentiated neurons leads to the accumulation of misfolded proteins and cell death, and provide a novel mechanism underlying neurodegeneration.

The genetic code is established in the aminoacylation reactions of aminoacyl-tRNA synthetases, where each amino acid is linked to its cognate tRNA that bears the anticodon triplet of the code. The rate of misincorporation of amino acids into proteins is very low (estimated at one error in every 10^3–10^4 codons)[1,2], and this high accuracy results largely from the precision of aminoacylation reactions. In addition to tRNA recognition, aminoacyl-tRNA synthetases must discriminate between amino acids in the cellular pool. Generally, amino acids with side chains that are bulkier than those of the cognate amino acids are sterically excluded from the active sites of tRNA synthetases, but smaller amino acids can fit into the active site pocket and be misactivated and mischarged. These misactivated adenylates or mischarged tRNAs are normally cleared by the editing function of aminoacyl-tRNA synthetases, encoded by a domain that is distinct from the domain for aminoacylation. If they are not cleared, genetic code ambiguity is introduced (that is, a given codon in the messenger RNA will specify incorporation of more than one amino acid, resulting in the production of 'statistical polypeptides')[3–6]. Here we report that an editing defect in a single tRNA synthetase in the mouse results in neurodegeneration associated with protein characteristics consistent with heterogeneous polypeptide production (Supplementary Fig. 1). These results provide a novel mechanism for the generation of misfolded proteins, which are associated with human diseases—many of which have neuron loss[7–9].

Purkinje cell loss in sticky mutant mice

The sticky (*sti*) mutation was identified by the rough, unkempt 'sticky' appearance of fur in mice homozygous for the mutation. As mice age, this rough coat is accompanied by follicular dystrophy and patchy hair loss (Supplementary Fig. 2). However, at six weeks of age mild tremors appear, which progress to overt ataxia (Supplementary Fig. 3). Histological analysis reveals a loss of cerebellar Purkinje cells in C57BL/6J.stock$^{sti/sti}$ (*sti*/*sti*) mice beginning at three weeks of age (Fig. 1a–g). By six weeks, extensive Purkinje cell loss is observed, particularly in the rostral cerebellum. This degeneration is slowly progressive so that most Purkinje cells degenerate over the course of a year, excluding the majority of these neurons in the caudally located lobule X.

To investigate the nature of Purkinje cell loss, we performed immunohistochemical studies with the apoptotic markers cleaved caspase 3 and cleaved poly(ADP-ribose) polymerase (PARP). Purkinje cells that were positive for these markers were observed in mutant, but not wild-type, animals at four weeks of age (Fig. 1h–j and data not shown). Further confirmation that these cells were undergoing apoptosis was obtained from TUNEL (TdT-mediated dUTP nick end labelling)-positive mutant Purkinje cells (Fig. 1k–m).

The *sti* mutation disrupts the *Aars* gene

A genome scan using polymorphic microsatellite markers on affected F_2 animals initially localized the *sti* mutation to chromosome 8. Further fine mapping demonstrated that *sti* resided in a 1.54-centimorgan (cM) region (45 recombinants, 2,932 meioses; Fig. 2a and Supplementary Fig. 4). Expression analysis of genes in the *sti* critical region failed to reveal any differences between wild-type and mutant cerebellar RNA. However, sequencing of complementary DNA revealed a C-to-A nucleotide change in the alanyl-tRNA synthetase gene (*Aars*) at nucleotide 2,201 of the transcript in mutant mice—predicted to cause an alanine to glutamic acid substitution at amino acid 734, a residue that is evolutionarily conserved (Supplementary Fig. 5).

To confirm that the mutation in the alanyl-tRNA synthetase protein (AlaRS) underlies Purkinje cell degeneration in *sti* mutant mice, we performed transgenic rescue experiments using a wild-type genomic DNA fragment containing the AlaRS coding region, and 7.3 kb and 1.7 kb of 5′ and 3′ flanking regions, respectively (Fig. 2b). We identified two founder lines with cerebellar expression of *Aars* at approximately five times that observed in wild-type animals (data not shown). Mutant *sti*/*sti* mice carrying the *Aars* transgene did not

[1]The Jackson Laboratory, 600 Main Street, Bar Harbor, Maine 04609, USA. [2]The Skaggs Institute for Chemical Biology, The Scripps Research Institute, 10550 North Torrey Pines Road, La Jolla, California 92037, USA. [3]Howard Hughes Medical Institute, Bar Harbor, Maine 04609, USA. †Present address: Department of Bioelectronics and Bioinformatics, Korea Bio Polytechnic College, Chungnam 320-905, Korea.

develop ataxia, and immunohistochemistry with calbindin-D28 demonstrated that the *sti*-associated degeneration of Purkinje cells was rescued by the transgene (Fig. 2c–f). These data demonstrate that wild-type AlaRS is necessary for Purkinje cell survival in the adult cerebellum.

Sensitivity to non-cognate amino acids

As shown in Fig. 3a, mouse AlaRS is 968 amino acids in length with a large amino-terminal catalytic domain (amino acids 1–561) for amino-acid activation and tRNA aminoacylation, and an evolutionarily conserved editing domain for hydrolytic editing of non-cognate amino acids (glycine or serine) from misaminoacylated $tRNA^{Ala}$ (refs 10, 11). Analysis of the primary structure of AlaRS suggested that Ala 734 lies within the putative editing domain (Fig. 3a). The area encompassing this residue (Fig. 3a, b (shown in purple)) has been shown to enhance aminoacylation efficiency but has no role in amino-acid activation in *Escherichia coli*[11]. The *sti* Ala–Glu substitution seems to be within a loop region well outside of the active site of the editing domain (>15 Å) but, nevertheless, within the sequence predicted to form this domain (Fig. 3b).

In *E. coli*, mutations within the AlaRS editing domain result in increased production of misacylated Gly-$tRNA^{Ala}$ or Ser-$tRNA^{Ala}$ (ref. 11). In addition to misacylation of $tRNA^{Ala}$, cell death occurs in editing-deficient strains grown in elevated serine or glycine[11]. To determine whether the *sti* mutation may confer sensitivity to amino acids that may be mischarged by the mutant AlaRS enzyme, we analysed the survival of mutant and wild-type mouse embryonic fibroblasts (MEFs) challenged by the addition of individual amino acids to the medium at levels 25× and 100× that of unaltered media (Fig. 3c–g). Despite slightly decreased viability of both *sti*/*sti* and wild-type fibroblasts at increasing concentrations of amino acids, no differences in cell viability were observed following the addition of alanine, histidine or methionine ($P > 0.05$). In contrast, serine dramatically increased cell death of *sti*/*sti* fibroblasts in a dose-dependent manner relative to that observed in wild-type cultures ($P < 0.0001$). Mutant fibroblasts were marginally sensitive to glycine (2.59 ± 1.22% versus 5.30 ± 1.19% cell death in wild-type versus mutant cells; values are mean ± s.e.m.). The specific sensitivity to serine is consistent with defective editing in the *sti* mutant AlaRS protein. Also, *sti*/+ fibroblasts show an increased sensitivity to serine that is intermediate to that of wild-type and *sti*/*sti* fibroblasts (Fig. 3h). This contrasts with the normal phenotype of *sti*/+ mice, suggesting that environmental challenges can result in gene dosage effects of the *sti* mutation.

Defects in editing of non-cognate amino acids from mischarged tRNAs should lead to misincorporation of these amino acids during protein synthesis, which would in turn lead to the accumulation of misfolded/unfolded proteins. To determine if serine-induced cell death in *sti*/*sti* cells is correlated with the accumulation of unfolded proteins, we analysed ubiquitination of proteins in serine-treated fibroblasts pretreated with mitomycin C to inhibit cell division and dilution of misfolded proteins (Fig. 3i). In the absence of serine addition, polyubiquitinated proteins were greatly increased in *sti*/*sti* fibroblasts, indicating that misfolded/unfolded proteins accumulate in these cells. Ubiquitinated proteins increased in both mutant and wild-type cells on addition of serine to the media, indicating that high concentrations of serine cause protein misfolding even in wild-type cells, perhaps by interfering with AlaRS editing. Consistent with misfolded protein elevation, levels of stress-inducible, cytosolic heat shock protein 72 (HSP72) were increased in *sti*/*sti* fibroblasts, and also increased on the addition of serine to wild-type cells (Fig. 3i).

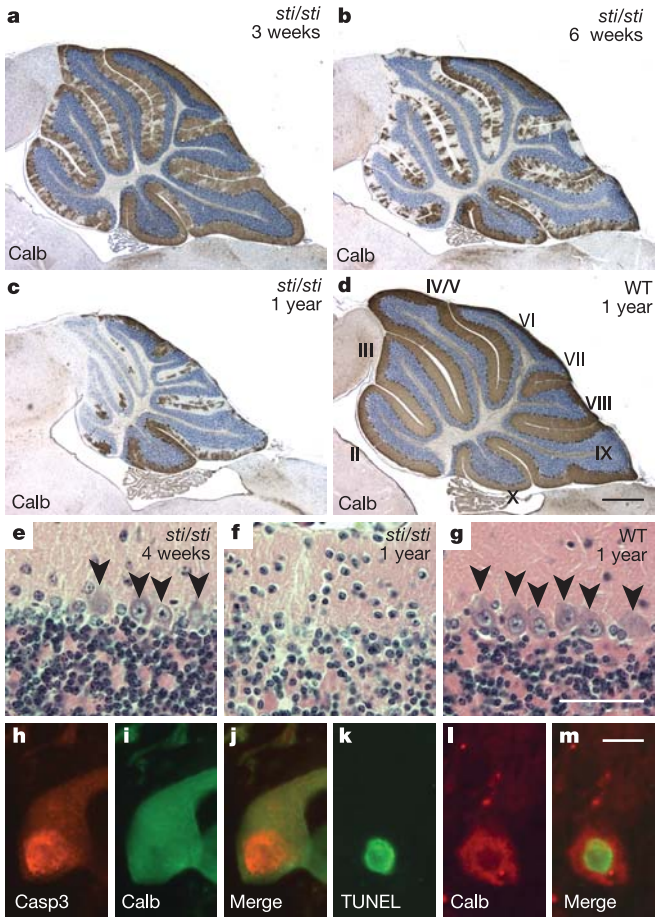

Figure 1 | Sticky mutant pathology. **a**–**d**, Calbindin D-28 (Calb) immunohistochemistry of sagittal sections of cerebella from 3-week-old (**a**), 6-week-old (**b**) or 12-month-old (**c**) *sti*/*sti* mutant and 12-month-old wild-type (WT) (**d**) mice. Cerebellar lobules are indicated by Roman numerals. **e**–**g**, Haematoxylin and eosin staining of Purkinje cells (arrowheads) in lobule II of cerebella from 1-month-old (**e**) or 12-month-old (**f**) *sti*/*sti* mutant and 12-month-old wild-type (**g**) mice. **h**–**m**, Cleaved caspase 3 (Casp3) immunohistochemistry (**h**–**j**) and TUNEL analysis (**k**–**m**) of 4-week-old mutant cerebella. Scale bars: **a**–**d**, 500 μm; **e**–**g**, 50 μm; **h**–**m**, 10 μm.

The *sti* mutation disrupts AlaRS editing

For functional analysis, we introduced the A734E mutation into both the mouse and the human enzyme, which is 92% identical (including Ala 734) to mouse AlaRS. Far-ultraviolet circular dichroism (far-UV CD) spectral analysis of purified wild-type and mutant proteins had identical minima and indistinguishable far-UV CD spectra, suggesting that the A734E substitution does not induce major changes in local secondary structure of AlaRS (Supplementary Methods and Supplementary Fig. 6).

A single G3:U70 acceptor stem base pair marks $tRNA^{Ala}$ throughout evolution for charging with alanine. As a consequence, AlaRS proteins from bacteria to humans charge $tRNA^{Ala}$ across species[12,13]. We analysed the effect of the A734E substitution on *in vitro* aminoacylation activity of human and mouse enzymes on *E. coli* $tRNA^{AlaGGC}$ or human $tRNA^{AlaUGC}$, respectively, both of which retain the G3:U70 base pair in the acceptor stem that is crucial for efficient AlaRS recognition[14]. Wild-type and mutant A734E human AlaRS purified from *E. coli* showed the same kinetics for aminoacylation for $tRNA^{Ala}$ (wild type: $k_{cat} = 1.5\,s^{-1}$ and $K_m = 5.7\,\mu M$; mutant: $k_{cat} = 1.6\,s^{-1}$ and $K_m = 6.8\,\mu M$). Similarly, no differences in aminoacylation kinetics were observed between recombinant wild-type ($k_{cat} = 1.5\,s^{-1}$ and $K_m = 0.49\,\mu M$) and mutant ($k_{cat} = 1.5\,s^{-1}$ and $K_m = 0.73\,\mu M$) mouse enzyme (Supplementary Fig. 7).

To test the effect of the *sti* mutation on editing, we assayed deacylation of mischarged $tRNA^{Ala}$ with mutant and wild-type enzyme. The viability of *sti* embryonic fibroblasts is more severely

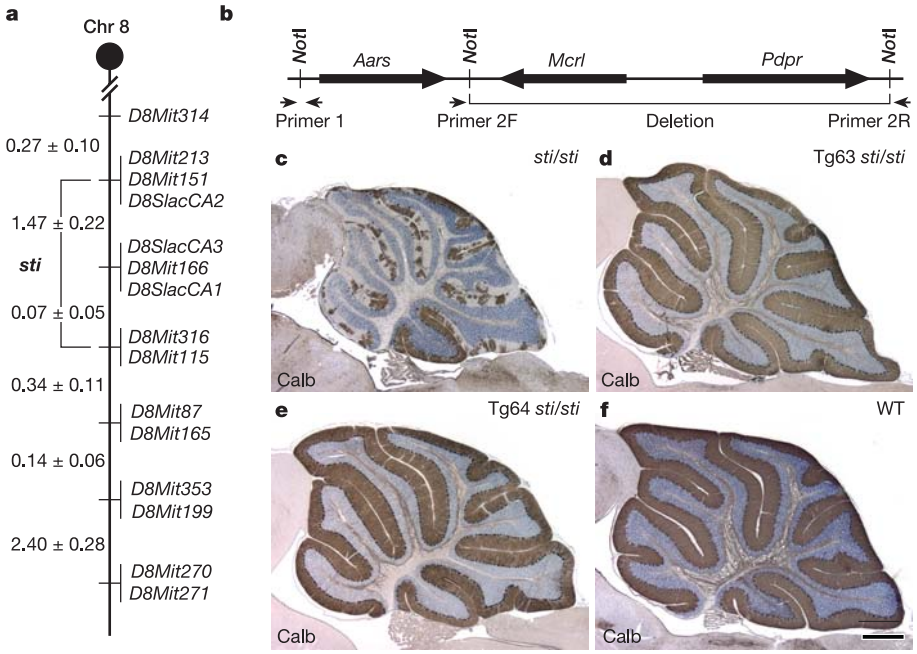

Figure 2 | The *sti* mutation is identified in the alanyl-tRNA synthetase (*Aars*) gene. **a**, The *sti* mutation was mapped to chromosome 8 (shown in cM ± s.e.m.). **b**, The RP24-359N5 bacterial artificial chromosome (BAC) contains the *Aars*, *Mrcl* and *Pdpr* genes, of which the latter two were deleted by partial digestion with *Not*I. Positions of primers used to genotype transgenic mice are shown. **c**–**f**, Immunohistochemistry of sagittal sections of cerebella from 3-month-old *sti*/*sti* (**c**), transgenic (Tg) *sti*/*sti* carrying the *Aars* transgene from line 63 or line 64 (**d**, **e**, respectively), and wild-type (**f**) mice using the calbindin D-28 antibody. Scale bar: 500 μm.

affected when challenged with serine than with glycine. Thus, we first examined the effect this mutation had on the ability of the enzyme to hydrolyse human Ser-tRNA^{Ala}. With the mutant enzyme, deacylation of Ser-tRNA^{Ala} was diminished by a reproducible 40–50% (Fig. 4a). In contrast, no deacylation of Ala-tRNA^{Ala} above background was observed with either mutant or wild-type enzyme, excluding the possibility of a loss in editing specificity by the *sti* mutant (Supplementary Fig. 8).

A loss of editing activity should result in the production and release of misacylated tRNAs. *In vivo*, these incorrect products are captured by elongation factors, delivered to the ribosome, and incorporated into nascent peptides. In the presence of the elongation factor (EF) EF-Tu to capture and sequester misacylated tRNA^{Ala}, a significantly higher accumulation of Ser-tRNA^{Ala} was observed in reactions using the mutant versus wild-type human enzyme (Fig. 4b). Although the deacylation of Ser-tRNA^{Ala} was nearly indistinguishable between the mutant and wild-type mouse enzymes, the mutant mouse enzyme also produced increased Ser-tRNA^{Ala} (Fig. 4c, d). Notably, although mouse AlaRS produces significant quantities of Ser-tRNA^{Ala}, it fails to generate Gly-tRNA^{Ala} (Supplementary Fig. 9),

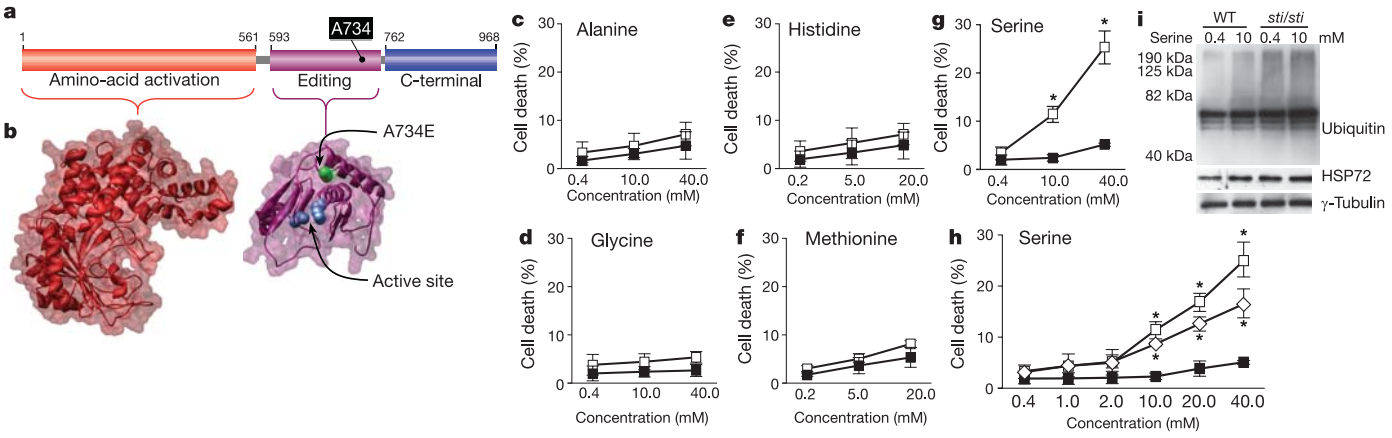

Figure 3 | Mutant fibroblasts are selectively sensitive to serine. **a**, **b**, AlaRS domains (**a**) and their three-dimensional structures (**b**). The amino-acid activation domain (red) and editing domain (purple) is modelled on *Aquifex aeolicus* AlaRS[34] and the *Pyrococcus horikoshii* free-standing AlaRS editing domain homologue[23], respectively. Blue spheres show the location of crucial active site residues. Ala 734 is depicted as a green sphere. **c**–**g**, Wild-type (black boxes) and mutant (open boxes) MEFs were treated with increasing concentrations of alanine (**c**), glycine (**d**), histidine (**e**), methionine (**f**) and serine (**g**). **h**, Viability curves for wild-type (black boxes), *sti*/+ (open diamonds) and *sti*/*sti* (open boxes) MEFs in the presence of increasing concentrations of serine. Values are the means of three or more independent experiments ±s.e.m. *, $P < 0.0001$. **i**, Western blot of extracts from mitomycin-C-arrested mutant and wild-type cells grown in unsupplemented (0.4 mM) or serine-supplemented (10 mM) media. Anti-γ-tubulin antibody was used as a loading control.

consistent with differential sensitivity of *sti*/*sti* embryonic fibroblasts to serine over glycine.

In vivo effects of decreased editing

The partial loss of editing function of A734E AlaRS and the accompanying increase in misacylated $tRNA^{Ala}$ would be predicted to result in the increased production of proteins with misincorporated amino acids, probably leading to the accumulation of misfolded proteins. Electron microscopy analysis of *sti*/*sti* cerebella revealed multilamellar membranous structures enveloping the cytoplasm and organelles, characteristic of autophagosomes (Fig. 5a–c). In addition, electron-dense globular structures, reminiscent of protein inclusions, were observed in the cytoplasm and perinuclear region of mutant Purkinje cells.

Ubiquitinated proteins are commonly found in neuronal inclusions in many neurodegenerative disorders[15]. Immunofluorescence for ubiquitin demonstrated intense punctate staining throughout the cytoplasm of *sti*/*sti* Purkinje cells that was not seen in the wild type (Fig. 5d–g). These puncta were also observed in the axons and dendrites of many Purkinje cells (data not shown). In addition, ubiquitin immunoreactivity was observed in the nucleolus of mutant Purkinje cells, suggesting that nucleolar proteins are also misfolded (Fig. 5h, i).

An increase in misfolded/unfolded proteins can result in the induction of molecular chaperones that bind to interactive surfaces of abnormal proteins and facilitate refolding or degradation of misfolded polypeptides[16–18]. Both cytoplasmic and endoplasmic-reticulum-localized members of the HSP70 chaperone family are associated with neuronal protein aggregates in many progressive neurodegenerative disorders[19]. Immunofluorescence for inducible, cytosolic HSP72 and constitutive, cytosolic heat shock cognate 70 (HSC70) demonstrated that these chaperones were induced in *sti* mutant Purkinje cells that also showed an increase in ubiquitinated proteins (Fig. 5j, k and Supplementary Fig. 10). Similarly, levels of the HSP70 co-chaperone HSP40 were markedly upregulated in these neurons (Supplementary Fig. 10).

Misfolded proteins within the endoplasmic reticulum can result in an imbalance between the unfolded protein load and the capacity of the endoplasmic reticulum protein folding machinery, also known as endoplasmic reticulum stress[20]. The intrinsic response to restore endoplasmic reticulum homeostasis is known as the unfolded protein response (UPR). To test whether the accumulation of unfolded proteins in *sti*/*sti* Purkinje cells results in endoplasmic reticulum stress, we examined the expression of the endoplasmic reticulum chaperone BiP (also known as GRP78 or HSPA5), and an endoplasmic-reticulum-stress-induced transcription factor CHOP (also known as GADD153 or DDIT3). Immunofluorescence analysis demonstrated that BiP is transiently upregulated in many Purkinje cells of the *sti*/*sti* cerebellum at two weeks of age compared with wild-type Purkinje cells where levels are very low (Supplementary Fig. 10). CHOP expression is apparent in mutant Purkinje cells, but not wild-type cells, by three weeks of age (Fig. 5l–o). It remains upregulated at five weeks of age, a time at which many Purkinje cells degenerate, indicating a potential role of CHOP in apoptosis, as previously suggested[21].

Discussion

Small amounts of misfolded proteins with abnormal conformations can serve to nucleate additional proteins, forming larger, potentially toxic, protein aggregates or leading to the loss of function of aggregated proteins[22]. Postmitotic cells, in particular neurons, seem to be extremely sensitive to misfolded proteins, possibly because these potentially toxic species cannot be diluted by cell division. Indeed, the most dramatic phenotype in *sti* mutant mice is neuron loss. Like most neurodegenerative diseases, pathology is only observed in

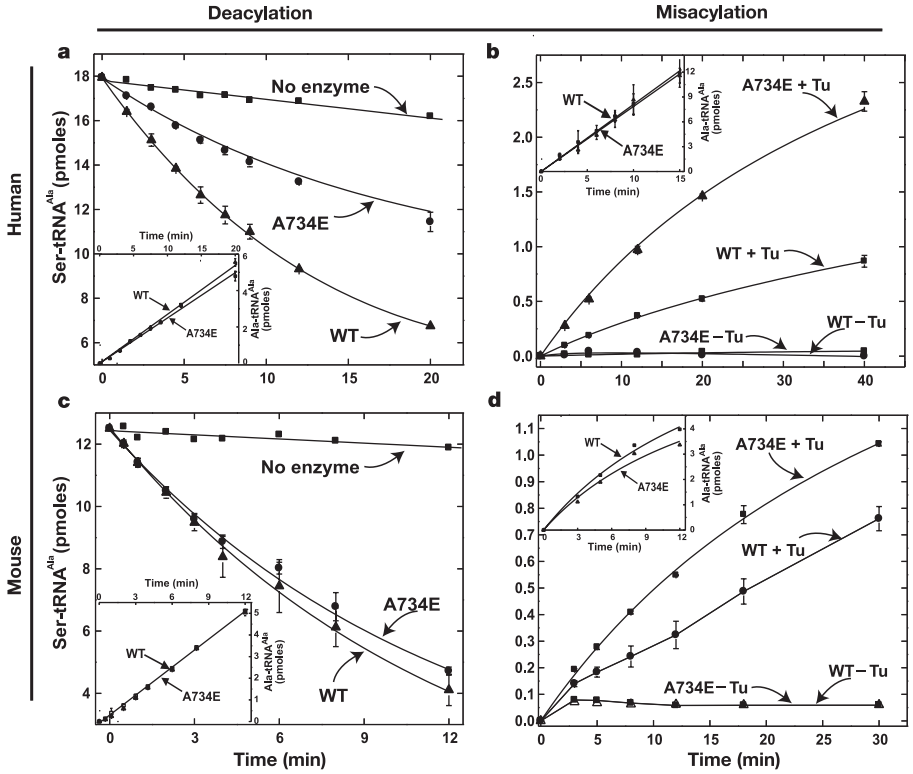

Figure 4 | Editing deficiency in *sti* mutant AlaRS. **a**, Deacylation of [^{3}H]Ser-$tRNA^{Ala}$ by wild-type or A734E human AlaRS. Inset, aminoacylation control with the same enzyme dilution used in the experiment shown in the main panel. **b**, Misacylation of $tRNA^{Ala}$ with serine by wild-type or A734E human AlaRS in the presence of *Thermus thermophilus* EF-Tu. Inset, aminoacylation dilution control. **c**, Deacylation of [^{3}H]Ser-$tRNA^{Ala}$ by mouse AlaRS. Inset, aminoacylation control with the same enzyme dilution used in the experiment shown in the main panel. **d**, Misacylation of $tRNA^{Ala}$ by mouse AlaRS. Inset, aminoacylation dilution control. Values are the means of two independent experiments ± s.d.

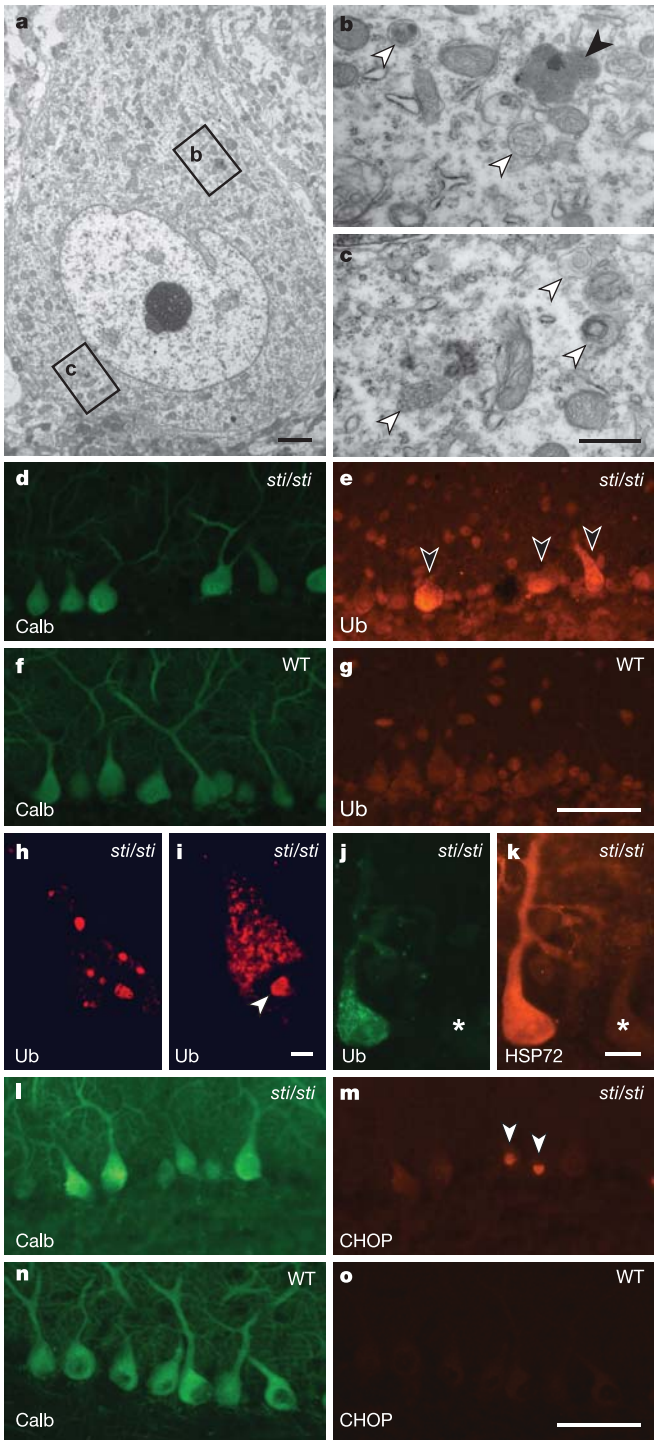

Figure 5 | Accumulation of misfolded proteins in *sti/sti* Purkinje cells. **a**–**c**, Electron micrographs of *sti*/*sti* Purkinje neurons at 3 weeks of age. Boxed areas in **a** are shown in detail in **b** and **c**. Autophagosome-like vacuoles (open arrowheads) and globular structures reminiscent of protein accumulations (closed arrowhead), are indicated. **d**–**g**, Immunofluorescence with antibodies to calbindin D-28 or ubiquitin (Ub) on 3-week-old wild-type or *sti*/*sti* cerebella. Arrowheads indicate punctate ubiquitin staining in the cytoplasm of mutant Purkinje cells. **h**, **i**, Confocal microscopy analysis of *sti*/*sti* Purkinje cells stained with ubiquitin antibodies demonstrates large puncta of staining throughout the cytoplasm and nucleolus (arrowhead). **j**, **k**, HSP72 staining is induced in cells with punctate ubiquitin staining. An asterisk indicates an adjacent Purkinje cell without punctate ubiquitin staining or induced expression of HSP72. **l**–**o**, Immunofluorescence of 3-week-old *sti*/*sti* (**l**, **m**) and wild-type (**n**, **o**) cerebella with CHOP (arrowheads) and calbindin D-28 antibodies. Scale bars: **a**, 2 μm; **b**, **c**, 500 nm; **d**–**o**, 50 μm.

specific neurons in *sti* mutant mice: in this case, the cerebellar Purkinje cells. The cause of this specificity is not clear. In the human and mouse, cytoplasmic AlaRS, like most tRNA synthetases, is encoded by a single gene, and a separate gene encodes the mitochondrial form. However, the mouse genome does contain AlaRS-like genes that encode proteins with free-standing tRNA synthetase editing domains. Although these proteins have been shown to edit mischarged tRNAs in prokaryotes[23,24], it is not known whether these function in a similar manner in eukaryotes, potentially compensating for the loss of AlaRS-mediated editing in other neuronal populations. Alternatively, Purkinje cells might be inherently less efficient at degrading misfolded proteins or more sensitive to the deleterious effects of these polypeptides, as suggested by the many human repeat-expansion diseases that are associated with ataxia and Purkinje cell loss[25]. Furthermore, recent studies in mouse and human demonstrate that the loss of the widely expressed co-chaperone of the endoplasmic reticulum chaperone BiP, SIL1, specifically results in misfolded proteins and subsequent degeneration of Purkinje cells[26–28].

Our data demonstrate the importance of proofreading of non-cognate amino acids by aminoacyl synthetases in terminally differentiated neurons. Although our results are most consistent with loss of editing activity, we cannot completely rule out the possibility that the *sti* mutation disrupts a novel function of AlaRS. However, our independent experiments have shown that inducible expression of an editing-defective valyl-tRNA synthetase in cultured mammalian cells leads to mistranslation and apoptosis, which is exacerbated by the addition to the culture of a non-canonical amino acid[35]. Furthermore, because editing domains of tRNA synthetases are functionally independent of those for the essential aminoacylation function, mild defects in editing could be transmitted from generation to generation without disruption of protein synthesis, raising the possibility that some heritable diseases are connected to mild mutations in tRNA synthetase editing functions that, in turn, generate misfolded proteins.

METHODS

Mice. The sticky mutation arose spontaneously in an unknown stock mouse and was transferred to a C57BL/6J background. The truncated RP24-359N5 BAC was microinjected into the pronuclei of C57BL/6J embryos. Transgenic mice were identified as described in the Supplementary Methods. An intersubspecific intercross (C57BL/6J.stock$^{sti/sti}$ × CAST/Ei) was used for genetic mapping.

Immunohistochemistry and electron microscopy. Electron microscopy studies, TUNEL assays, immunohistochemistry and immunofluorescence were performed as described previously[28,29], or using antibodies to HSC70, HSP72 and HSP40 (Stressgen Bioreagents; 1:200 dilution).

Mouse embryonic fibroblast cultures. MEFs were prepared by standard protocols[30]. Amino acids were added to the culture media for 24 h; cells were collected and stained with propidium iodide. The percentage of cell death was measured by fluorescence-activated cell sorting (FACS) analysis. Statistical significance was determined by analysis of covariance (ANCOVA) using SAS software (SAS Institute).

Western blots. MEFs were treated with mitomycin C (1 μg ml^{-1}) for 2 h, before a 24-h incubation in serine-supplemented media. Blots were incubated with antibodies to ubiquitin (Cell Signalling; 1:1,000), HSP72 (Stressgen Bioreagents; 1:1,000) and γ-tubulin (Sigma; 1:2,000).

Aminoacylation, deacylation and misacylation assays. Overexpression and purification of *E. coli* tRNA^{AlaGGC} and human tRNA^{AlaUGC} was accomplished as described[31]. Purified human tRNA^{AlaUGC} (34 μM) was aminoacylated by *E. coli* AlaRS (C666A/Q584H) as described[11]. Deacylation assays were performed at pH 7.5, 26 °C as described[11,32], using human or mouse (8 nM and 2 nM, respectively) wild-type mutant A734E AlaRS, and 6.2 μM mischarged tRNA^{Ala}. Misacylation assays were performed at pH 7.5, 26 °C using human or mouse (1.3 μM and 3.7 μM, respectively) wild-type or mutant A734E AlaRS, 10 μM serine (or 8.8 μM glycine), 10 μM, tRNA^{Ala}, 4 mM ATP, 4 μM *Thermus thermophilus* EF-Tu, and 4 ng μl^{-1} of inorganic pyrophosphatase (Roche) in EF-Tu buffer[11,33]. EF-Tu was activated as described[33].

Received 3 February; accepted 19 July 2006.
Published online 13 August 2006.

1. Loftfield, R. B. & Vanderjagt, D. The frequency of errors in protein biosynthesis. *Biochem. J.* **128**, 1353–1356 (1972).

2. Jakubowski, H. & Goldman, E. Editing of errors in selection of amino acids for protein synthesis. *Microbiol. Rev.* **56,** 412–429 (1992).
3. Bacher, J. M., de Crecy-Lagard, V. & Schimmel, P. R. Inhibited cell growth and protein functional changes from an editing-defective tRNA synthetase. *Proc. Natl Acad. Sci. USA* **102,** 1697–1701 (2005).
4. Doring, V. *et al.* Enlarging the amino acid set of *Escherichia coli* by infiltration of the valine coding pathway. *Science* **292,** 501–504 (2001).
5. Nangle, L. A., de Crecy-Lagard, V., Doring, V. & Schimmel, P. Genetic code ambiguity. Cell viability related to the severity of editing defects in mutant tRNA synthetases. *J. Biol. Chem.* **277,** 45729–45733 (2002).
6. Pezo, V. *et al.* Artificially ambiguous genetic code confers growth yield advantage. *Proc. Natl Acad. Sci. USA* **101,** 8593–8597 (2004).
7. Selkoe, D. J. Folding proteins in fatal ways. *Nature* **426,** 900–904 (2003).
8. Dobson, C. M. Protein folding and misfolding. *Nature* **426,** 884–890 (2003).
9. Ross, C. A. & Poirier, M. A. Protein aggregation and neurodegenerative disease. *Nature Med.* **10** (Suppl.), S10–S17 (2004).
10. Dock-Bregeon, A. *et al.* Transfer RNA-mediated editing in threonyl-tRNA synthetase. The class II solution to the double discrimination problem. *Cell* **103,** 877–884 (2000).
11. Beebe, K., Ribas De Pouplana, L. & Schimmel, P. Elucidation of tRNA-dependent editing by a class II tRNA synthetase and significance for cell viability. *EMBO J.* **22,** 668–675 (2003).
12. Hou, Y. M. & Schimmel, P. Evidence that a major determinant for the identity of a transfer RNA is conserved in evolution. *Biochemistry* **28,** 6800–6804 (1989).
13. Ripmaster, T. L., Shiba, K. & Schimmel, P. Wide cross-species aminoacyl-tRNA synthetase replacement *in vivo*: yeast cytoplasmic alanine enzyme replaced by human polymyositis serum antigen. *Proc. Natl Acad. Sci. USA* **92,** 4932–4936 (1995).
14. Hou, Y. M. & Schimmel, P. A simple structural feature is a major determinant of the identity of a transfer RNA. *Nature* **333,** 140–145 (1988).
15. Ross, C. A. & Pickart, C. M. The ubiquitin–proteasome pathway in Parkinson's disease and other neurodegenerative diseases. *Trends Cell Biol.* **14,** 703–711 (2004).
16. Welch, W. J. Role of quality control pathways in human diseases involving protein misfolding. *Semin. Cell Dev. Biol.* **15,** 31–38 (2004).
17. Dobson, C. M. Principles of protein folding, misfolding and aggregation. *Semin. Cell Dev. Biol.* **15,** 3–16 (2004).
18. Barral, J. M., Broadley, S. A., Schaffar, G. & Hartl, F. U. Roles of molecular chaperones in protein misfolding diseases. *Semin. Cell Dev. Biol.* **15,** 17–29 (2004).
19. Muchowski, P. J. & Wacker, J. L. Modulation of neurodegeneration by molecular chaperones. *Nature Rev. Neurosci.* **6,** 11–22 (2005).
20. Xu, C., Bailly-Maitre, B. & Reed, J. C. Endoplasmic reticulum stress: cell life and death decisions. *J. Clin. Invest.* **115,** 2656–2664 (2005).
21. Zinszner, H. *et al.* CHOP is implicated in programmed cell death in response to impaired function of the endoplasmic reticulum. *Genes Dev.* **12,** 982–995 (1998).
22. Murphy, R. M. Peptide aggregation in neurodegenerative disease. *Annu. Rev. Biomed. Eng.* **4,** 155–174 (2002).
23. Sokabe, M., Okada, A., Yao, M., Nakashima, T. & Tanaka, I. Molecular basis of alanine discrimination in editing site. *Proc. Natl Acad. Sci. USA* **102,** 11669–11674 (2005).
24. Ahel, I., Korencic, D., Ibba, M. & Soll, D. Trans-editing of mischarged tRNAs. *Proc. Natl Acad. Sci. USA* **100,** 15422–15427 (2003).
25. Gatchel, J. R. & Zoghbi, H. Y. Diseases of unstable repeat expansion: mechanisms and common principles. *Nature Rev. Genet.* **6,** 743–755 (2005).
26. Senderek, J. *et al.* Mutations in *SIL1* cause Marinesco–Sjogren syndrome, a cerebellar ataxia with cataract and myopathy. *Nature Genet.* **37,** 1312–1314 (2005).
27. Anttonen, A. K. *et al.* The gene disrupted in Marinesco–Sjogren syndrome encodes SIL1, an HSPA5 cochaperone. *Nature Genet.* **37,** 1309–1311 (2005).
28. Zhao, L., Longo-Guess, C., Harris, B. S., Lee, J. W. & Ackerman, S. L. Protein accumulation and neurodegeneration in the woozy mutant mouse is caused by disruption of SIL1, a cochaperone of BiP. *Nature Genet.* **37,** 974–979 (2005).
29. Ackerman, S. L. *et al.* The mouse rostral cerebellar malformation gene encodes an UNC-5-like protein. *Nature* **386,** 838–842 (1997).
30. Hogan, B. *Manipulating the Mouse Embryo: A Laboratory Manual* (Cold Spring Harbor Laboratory Press, Cold Spring Harbor, New York, 1986).
31. Xue, H., Shen, W. & Wong, J. T. Purification of hyperexpressed *Bacillus subtilis* $tRNA^{Trp}$ cloned in *Escherichia coli*. *J. Chromatogr.* **613,** 247–255 (1993).
32. Beebe, K., Merriman, E., Ribas De Pouplana, L. & Schimmel, P. A domain for editing by an archaebacterial tRNA synthetase. *Proc. Natl Acad. Sci. USA* **101,** 5958–5963 (2004).
33. Pleiss, J. A. & Uhlenbeck, O. C. Identification of thermodynamically relevant interactions between EF-Tu and backbone elements of tRNA. *J. Mol. Biol.* **308,** 895–905 (2001).
34. Swairjo, M. A. *et al.* Alanyl-tRNA synthetase crystal structure and design for acceptor-stem recognition. *Mol. Cell* **13,** 829–841 (2004).
35. Nangle, L. A., Motta, C. M. & Schimmel, P. Global effects of mistranslation from an editing defect in mammalian cells. *Chem. Biol.* (in the press).

Supplementary Information is linked to the online version of the paper at www.nature.com/nature.

Acknowledgements We thank The Jackson Laboratory sequencing, microchemistry, histology, bioimaging and microinjection services for their contributions. We also thank L. Dionne and K. Seburn for rotorod testing and data analysis, J. Szatkiewicz for assistance with statistical analysis, J. Torrance for graphics assistance, P. O'Maille, W. Waas and A. Wolfson for gifts of plasmids, and C. Motta and E. Merriman for facilitating the expression and purification of proteins. We are also grateful to the laboratory of J. Kelly for CD spectrometer assistance and to R. Burgess and P. Nishina for comments on the manuscript. This work was supported by grants from the National Institute of Neurological Disorders and Stroke and the National Institute on Aging to S.L.A., the National Institute of General Medical Sciences and a fellowship from the National Foundation for Cancer Research to P.S., a grant from the National Center for Research Resources to M.T.D., and an institutional National Cancer Institute core grant (JAX). S.L.A. is an investigator of the Howard Hughes Medical Institute.

Author Contributions J.W.L. designed and performed mouse and cell culture experiments, K.B. and L.A.N. designed and performed biochemical analyses, J.J. performed mutation analysis, M.T.D. provided the congenic *sti* mice and oversaw initial mapping experiments, S.A.C. and C.M.L.-G. performed genetic mapping experiments, J.P.S. performed hair pathological analysis, P.S. and S.L.A. designed and supervised experiments. All authors discussed the results and commented on the manuscript, which was written by J.W.L., K.B., P.S. and S.L.A.

Author Information The sequence for mouse *Aars* has been deposited in GenBank under the accession number AY223875; sequence-tagged sites (STSs) for *D8SlacCA1* (DQ386090), *D8SlacCA2* (DQ386088) and *D8SlacCA3* (DQ386089) can also be found in GenBank. Reprints and permissions information is available at www.nature.com/reprints. The authors declare no competing financial interests. Correspondence and requests for materials should be addressed to S.L.A. (susan.ackerman@jax.org).